A sub-40nm nanostructured $La_{0.7}Sr_{0.3}MnO_3$ planar magnetic memory

T. Arnal[*], M. Bibes[*], Ph. Lecoeur[*], B. Mercey[**], W. Prellier[**] and A.M. Haghiri-Gosnet[*]

[*] Institut d'Electronique Fondamentale, IEF/ UMR 8622, Université Paris Sud,
Bâtiment 220, 91405 Orsay Cedex, France, anne-marie.haghiri@ief.u-psud.fr
[**] CRISMAT – Laboratoire de Cristallographie et Sciences des Matériaux,
6 Boulevard du maréchal Juin, 14050 Caen Cedex, France, bernard.mercey@ismra.fr

ABSTRACT

A single-step nanolithography planar process, which allows generating the core-element of a spin-polarized magnetic memory in the fully spin-polarized $La_{0.7}Sr_{0.3}MnO_3$ (LSMO) manganite, is reported. Taking benefit of the proximity effects due to backscattered electrons, a conventional electron-beam patterning process at 30 KeV has been optimized to generate sub-50 nm-wide nanokinks in the magnetic microbridge. The best layout for the nanokinks, the electron beam patterning parameters and the results of the ion beam etching (IBE) for transferring these nanopatterns in the magnetic oxide are reported.

Keywords: spintronics, manganite, nanolithography, MRAM.

1 INTRODUCTION

Due to their large spin polarisation [1], ferromagnetic oxides, such as $La_{0.7}Sr_{0.3}MnO_3$ (LSMO), Fe_3O_4 and CrO_2, are promising materials for spin-electronics and can be used as injectors of spin-polarised electrons in magnetic memories. Also, their peculiar transport properties across interfaces, like tunnel junctions [2-3] and domain walls [4] allow an enhancement of the magneto-resistive response at low fields in memories applications.

The introduction of a nanometric constriction inside a thin ferromagnetic film has several effects, such as the pinning at this constriction of a domain wall (DW) [5]. Upon crossing a thin DW, the spin of the electrons cannot maintain a parallel alignment with the local magnetization, which can induce a large increase of the resistance [6]. If a magnetic field is applied or a pulsed current is injected, the DW can move and thus disappear. A large MR effect can be observed and gigantic values should be recorded in a half-metal. The challenge is thus to pattern and to etch these highly polarized half-metallic oxides in a sub-50 nm range.

We report on the optimization of the single-step nanolithography planar process that allows generating the core-element of a spin-polarized magnetic memory in $La_{0.7}Sr_{0.3}MnO_3$ (LSMO). Comparatively to conventional vertical tunnel junctions, this approach is easier for growth, since it is based on a single layer of LSMO. The best geometry for the nanokinks will be first discussed based on dynamic micromagnetic simulations of the magnetization reversal under the application of magnetic field. This paper will then focus on the planar process, that allows to create nanokinks in the oxide film using a conventional single-step 30 KeV electron beam lithography (EBL) (nanokinks and bridge are patterned at the same process level). It will be demonstrated that sub-40 nm wide nanokinks can be patterned in routine in $La_{0.7}Sr_{0.3}MnO_3$ microbridge by taking advantages of the EBL proximity effects.

2 PRINCIPLE OF THE DEVICE

The concept of the planar memory is schematically described in the Figure 1-a). At the center of the bridge, two couples of straight nanokinks isolate a single magnetic monodomain that exhibits a high shape anisotropy along the direction of the field. Magnetization will thus rotate at higher field values in this central part generating a bistable MR response for intermediate fields.

For proper operation of the device, the whole track should be free of undesired pinning centers like grain-boundaries. Therefore, this study requires first epitaxial LSMO thin films of high cristallinity. The epitaxial 40nm-thick LSMO films have been grown on (100)-oriented

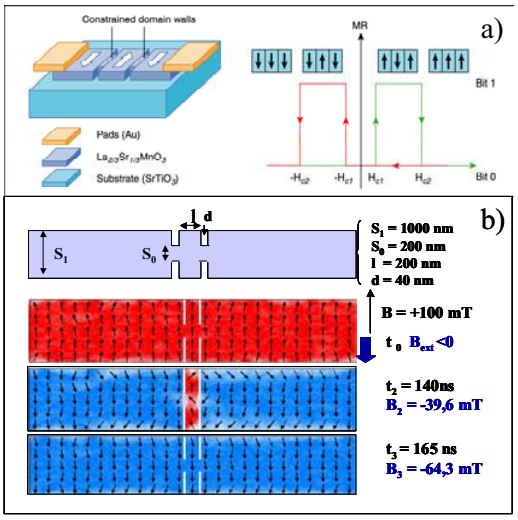

Figure 1 – a) principle of the planar memory with the MR response during reversal of the magnetization, b) micromagnetic simulations showing the pinning of two domain walls at the nanokinks for intermediate fields.

$SrTiO_3$ (STO) substrates using an original low-pressure Pulsed Laser Deposition (PLD) system (λ=248nm) at a reduced substrate temperature of 630 °C and under a low oxygen/ozone pressure of $5x10^{-3}$ mbar. The ozone concentration in the O_2/O_3 mixture ensures a full oxidation of the structure during growth. Details on the films deposition will be published elsewhere [7]. From our microstructural study, such epitaxial films appear free of any defect with a perfect "cube-on-cube" epitaxy, with an average grain-size larger than 1 µm. The surface roughness, deduced from AFM measurements, is about 0.2nm, i.e. half one unit cell. This exceptional flatness confirms the 2D step edge growth mode observed *in-situ* on the streaky RHEED patterns.

Dynamical micromagnetic simulations have been performed in order to determine the best geometry for both the kinks and the central domain. The Landau-Lifschitz equation has been resolved using the software *Oommf*. The thin film parameters were previously deduced from both SQUID and magneto-optical Kerr effects (MOKE) measurements. Note that the easy axes for magnetization are <110> and <1¯10> in the plane [8] and that the bridge is aligned along one of this axis. At 4K, the film parameters are: the saturation moment M_S = 5800 A/m (3.67 μ_B/f.u), the stiffness constant A = 1.84 10^{-12} J/m , the anisotropy coefficient K_1 = -3 10^5 erg/cm^3 (K_2 = 0 with the <001> direction as a pure hard axis) and the damping coefficient α = 0.5. The pinning of DW occurs only if the lateral thickness **d** of the kink is lower than 40 nm, as well as if the central domain is smaller than 200 nm (see Fig. 1 – b)).

3 EXPERIMENTAL

A first level for large Cr/Au contact pads and alignment cross-marks is elaborated using UV lithography. Pads are aligned along <110>.

During the second step, the bridge and the nanokinks are patterned simultaneously. This high resolution nanopatterning is performed using a 30KeV SEMFEG microscope equipped with a beam-scanning system and coupled with a computer-assisted design software ELPHY (from Raith company). Exposures on the single 300nm-thick layer of 950 k molecular weight polymethyl - polymethacrylate (PMMA) organic resist were carried out with a beam diameter of approximately 1 nm and with a minimal beam current of 13 pA. Note that the adjustment of focus and the correction of astigmatism were performed by observing at high magnification a small contamination dot of several nanometers in diameter. The current was measured using a small Faraday cell placed near the sample. The exposure time per pixel was fixed at 15 µs and the pixel-to-pixel distance was of 13.7 nm, corresponding to a writing speed lower than 1 nm/s. All the electronic doses have been normalized to the value of D = 1 = 140 µC/cm^2. A conventional development of 2.5 minutes was performed in a mixture 1:3 of methyl-isobutyl-ketone (MIBK) / isopropylic alcohol (IPA). No ultra-sonic agitation [9] was used for this conventional process and the samples are gently rinsed in pure IPA during 2 min.

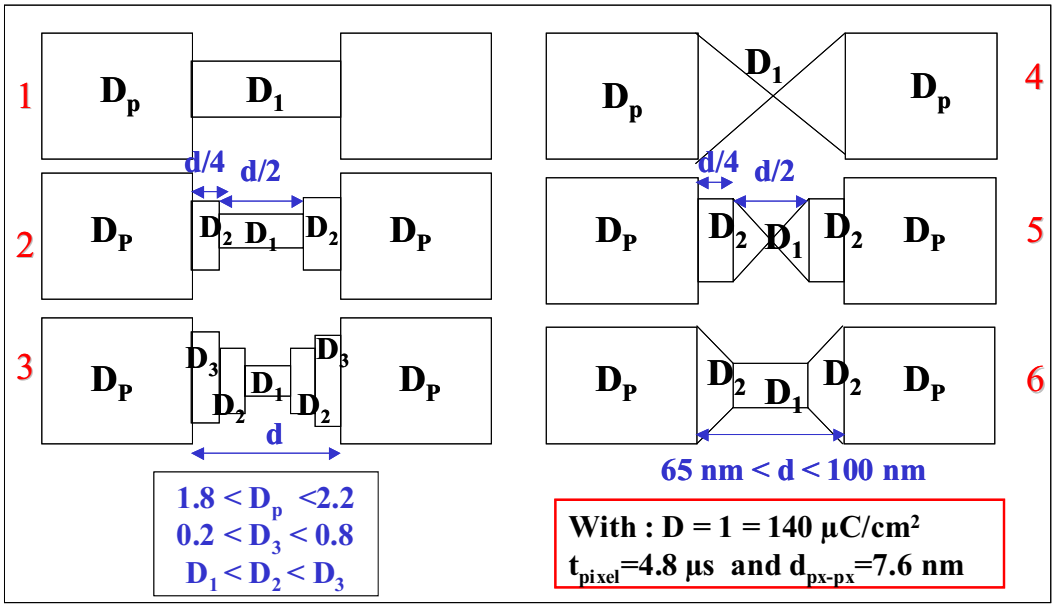

Figure 2 – Design of the six different geometries for the elaboration of the nanokinks (d is the width of the kink pattern). D_P and D_I are respectively the electronic doses of the bridge and of the kink. Note that for a better understanding, the dimensions of the patterns are not been reproduced at the exact scale: the width d of the nanokinks has been widely broadened.

The Al metallic mask for etching is evaporated and the nanopatterns are transferred to the LSMO film by an argon ion beam etching (IBE). During IBE, the sample holder was rotating and tilted at 45° to produce vertical profiles. The voltage and the current density of ions were fixed respectively at 500 V and 0.5 mA/cm^2. Finally, small Pt contacts lines are patterned on top of the nanostructured bridge in a 4-points configuration. The devices are inspected using a SEM imaging mode at a high magnification (> x50000) to precisely determine the final size of the nanokinks.

4 RESULTS AND DISCUSSION

Six different geometries have been tested for generating the nanokinks. These different designs are presented in the Figure 2. For these resolution tests, the total length of the bridge and its width are respectively 5 µm and 1 µm. The lateral thickness **d** of the kink is varied in the range 65 nm - 100 nm. In the geometries n°1, 2 and 3 (see figure 2), the kink has been cut out with lateral stripes. To take benefit of the proximity effects observed between the two large adjacent rectangles of the bridge, electron doses were decreased in these lateral stripes ($D_1<D_2<D_3$). For the geometries n°4, 5 and 6, the nanokinks has been divided using both rectangular and triangular-shape patterns.

Let us first consider the simplest geometry n°1 that is the conventional one. Because of the proximity effects of the 1µmx2.5µm rectangles, the width of the kink after development is around 40nm for a $d_{pattern}$ = 65 nm. To get a kink with the exact designed length (0.35 µm), doses for both the rectangles and the kink should be fixed at the optimal values D_p = 2 (280 µC/cm^2) and D_l ~ 0.4 (56 µC/cm^2). Under these conditions, the kink is 40 nm – wide. This corresponds to a 38% lateral reduction, which traduces the strong importance of the proximity effects, due to backscattered electrons from LSMO surface under PMMA resist.

The kink has the appearance of a small resist bridge in suspension over the LSMO surface (Fig.3a-geometry n°1). The fragile nanobridge will act as a mask during the Al evaporation allowing the transfer towards a kink during the Al lift-off process. The shape of the fragile nanobridge has been then optimized using the six different geometries. Figure 3-a) gives tilted SEM images of the kink which allows a direct observation of the resist nanobridge profiles. It is shown that the geometry n°5 produces the strongest bridge: the nanobridge exhibits long feet for a better strength and preserves the desired 0.35 µm length. The strength of such "geometry n°5" nanobridges has been confirmed during the Al lift-off process, since the lateral width of the transferred in Al kink approaches the measured value after development.

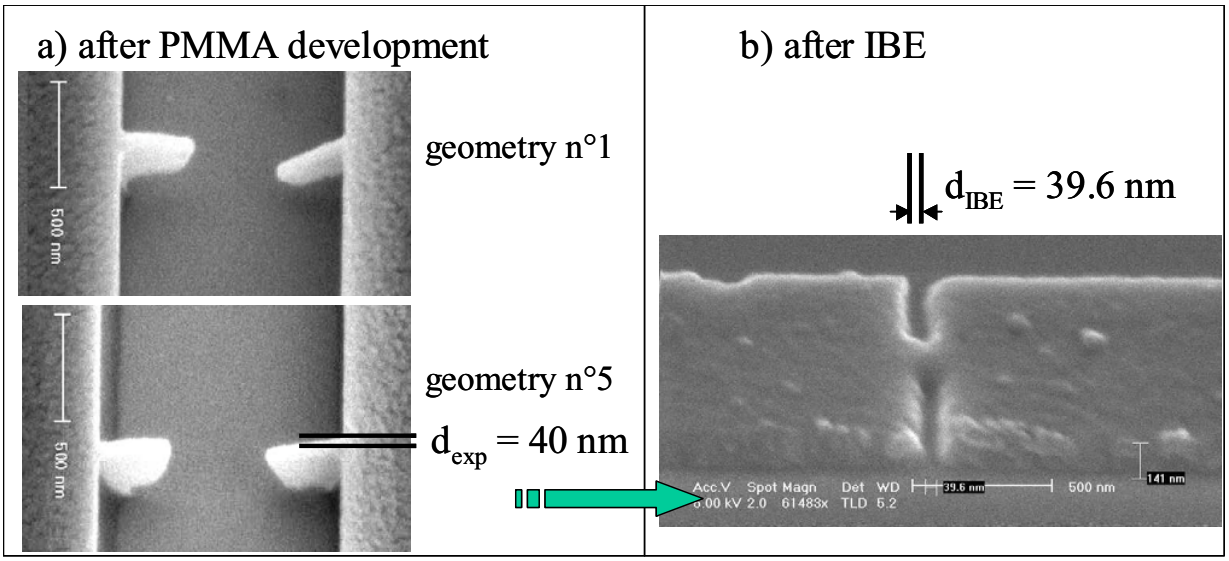

Figure 3 – Optimization of the shape of the nanobridge: a) tilted SEM images of the PMMA nanobridge after conventional development of the resist on top of the LSMO. The geometry n°5 appears to be the best way to get a strong bridge with large feet – b) SEM image of the geometry n° 5 nanokink that has been transferred in the LSMO thin film using IBE at 500 Volts.

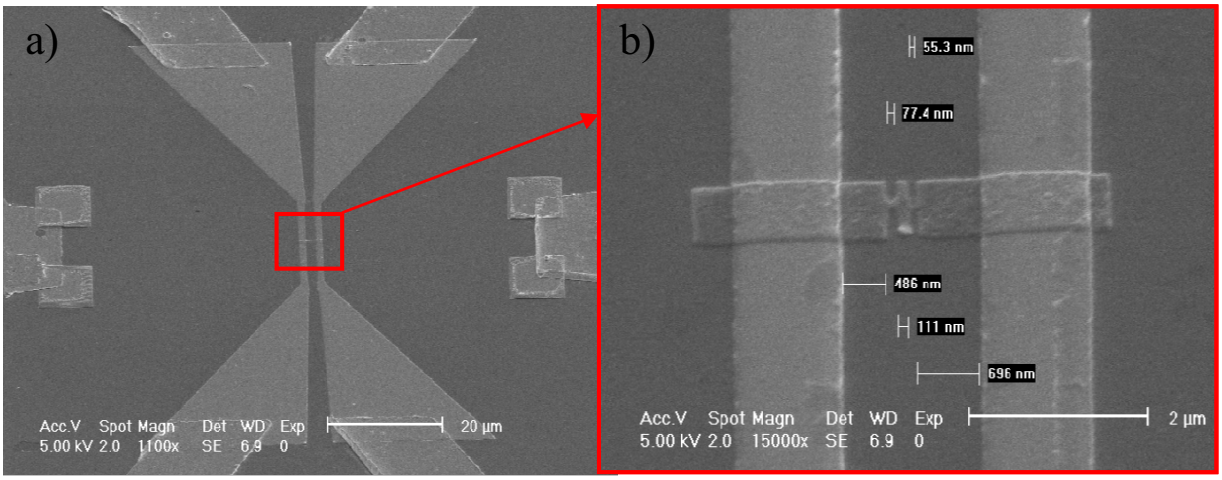

Figure 4 – a) a general top SEM view of the device after the last level of contact pads and b) a zoom of the central part of the nanostructured LSMO bridge. Note the two couples of kinks with lateral d values of d= 55 nm to 75 nm.

The majority of manganite nanodevices are ordinarily etched using conventional Ar ion beam etching (IBE) after an Al lift-off process. Al is preferred due to its high reactivity with oxygen. The bilayer Al / Al_2O_3 offers the best selectivity of about 2 for IBE of manganites. To avoid removal of the Al mask in solutions, which always attack the manganite film, the etching time is larger than the required time for a total Al etching. The kink transferred in LSMO by IBE is presented in the Figure 3-b) for the optimal geometry (n°5). No lateral reduction is observed between the PMMA development and the IBE process: the kinks exhibit the same width value of ~40 nm than the one of the nanobridge after development. This important result confirms first that both our lift-off and IBE processes are fully optimized for preserving lateral dimensions. Figure 4 gives both an overview of one device with its pads after the third contact level, as well as a zoom of the central domain with ~50nm-wide nanokinks.

5 CONCLUSION

Due to an optimized electron-beam pattern design, 40 nm-wide kinks have been successfully transferred in LSMO thin film, from a standard EBL process at 30 KeV. Proximity effects produce an interesting lateral reduction of the nanokink of around 40%.

The use of negative resist with a sufficiently high resolution will be tested in the future, in order to avoid the small over-etching for Al. The suppression of Al in the process should prevent the top surface of the manganite of a small reduction of oxygen. Moreover, the negative resist mask can leave on the device after the complete process for further etching to narrow the constrictions.

REFERENCES

[1] J.H.Park, E.Vescovo, H.J.Kim, C.Kwon, R.Ramesh, T.Venkatesan, Nature 392, 794, 1998.
[2] M. Bowen, M. Bibes, A. Barthélémy, J.-P. Contour, A. Anane, Y. Lemaitre, A. Fert, App. Phys. Lett 82, 233, 2003.
[3] Y Lu, X W Li, G Q Gong, G Xiao, A Gupta, Ph Lecoeur, J-Z Sun, Y Y Wang, V P Dravid, Phys. Rev. B 54, R8357, 1996.
[4] J Wolfman, A-M Haghiri-Gosnet, B Raveau, C Vieu, E Cambril, A Cornette, H Launois, J. Appl. Phys. 89, 6955, 2001.
[5] P. Bruno, Phys. Rev. Lett. 83, 2425, 1999.
[6] M. Viret, Y. Samson, P. Warin, A. Marty, F. Ott, E. Sondergard, O. Klein, C. Fermon, Phys. Rev. Lett. 85, 3962, 2000.
[7] Ph. Lecoeur and B. Mercey, to be published.
[8] A.M. Haghiri-Gosnet, J. Wolfman, B. Mercey, Ch. Simon, Ph. Lecoeur, M. Korzenski, M. Hervieu, R. Desfeux, G. Baldinozzi, J. Appl. Phys. 88, 4257, 2000.
[9] S. Yasin, D.G. Hasko, H. Ahmed, App. Phys. Lett 78, 2760, 2001.